Operator aliasing heuristics

John C. Bancroft

ABSTRACT

Aliasing of migrated data can be caused by the input data, the migration algorithm, or the migration parameters. This paper describes the aliasing caused by the Kirchhoff operator in a heuristic manner.

START WITH A SIMPLE WAVELET

The spectrum of the wavelet is zero at the lower frequencies; therefore, the sum of the samples will be zero.

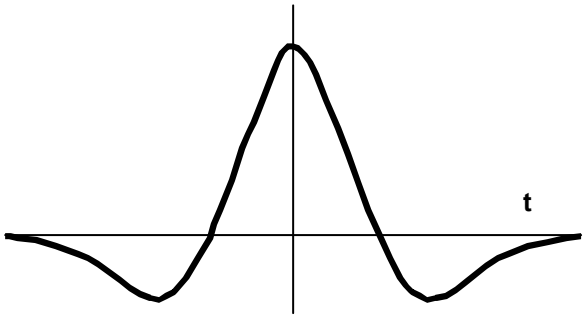

Figure 1

The following cartoon section (*x, t*) in Figure 2 contains one horizontal event with the wavelet described in Figure 1. Assume the data is continuous (very small samples in x and t) with the black band representing the positive amplitudes and the gray bands the negative amplitudes.

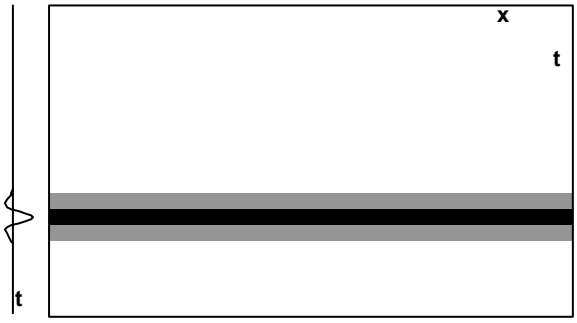

Figure 2

Figure 3 contains lines that intersect the event, with each containing a projection of the wavelet. The summation of these projected wavelets will also be zero after crossing the event. These lines will be used later to represent portions of diffraction curves as they cross the interface.

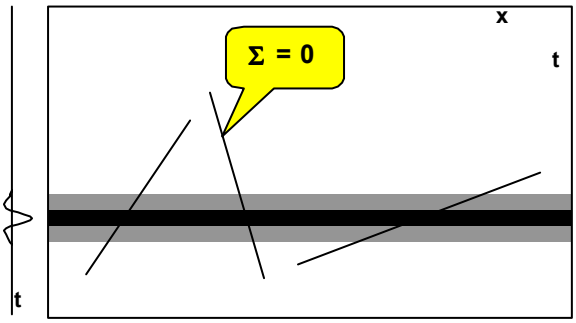

Figure 3

THE MIGRATION OPERATOR

After migration, a horizontal reflector should remain at the same location and have the same wavelet. There should be no additional energy above or below the event. When the diffraction is below the event, there will be no energy summed. An event above the diffraction will collect the energy in the projected wavelet that will sum to zero. A diffraction whose apex is in the event will sum energy that does not cancel and will reconstruct the original event. Note that we have assumed a continuous event that represents the wavelet at any intersection.

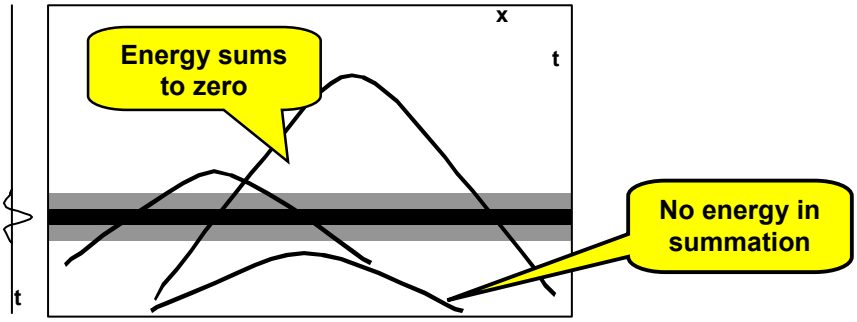

Figure 4. Continuum of traces

SPATIALLY SAMPLE DATA

Now, consider data that is spatially sampled with a visible space between the traces. Figure 5 shows the energy of the event on these traces.

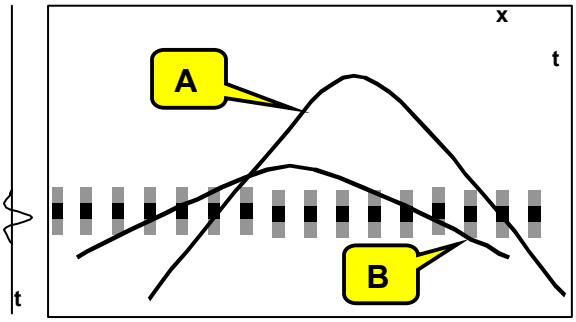

Figure 5. Energy from the event confined to traces.

The diffractions *A* and *B* in Figure 5 also intersect the event but don't pick up all the energy of the wavelet. Diffraction *A* will only pick up the maximum peak energy as it crosses the event. There are no other wavelet samples to cancel the summed energy. This summed energy will be placed at the apex of the diffraction. Other diffractions in the area of *A* will also pick up energy and produce an apparent event or noise well above the original event, i.e. aliased noise.

Diffraction *B* has a shallower dip as it crosses the event and picks up energy from a number of traces. If *B* crosses the event with enough trace intersections to represent the wavelet, then the sum will tend to zero.

If there were more traces with shorter trace intervals, then it might be possible for the diffraction at A to sum over a number of traces and the aliased energy will be reduced or eliminated. Consequently there is a relationship between the number of traces and the slope of the diffraction when it crosses the event.

Lowering the frequency of the wavelet in Figure 6 allows diffraction *A* to sum to zero as the wavelet is defined along the dipping intersection as highlighted by the oval.

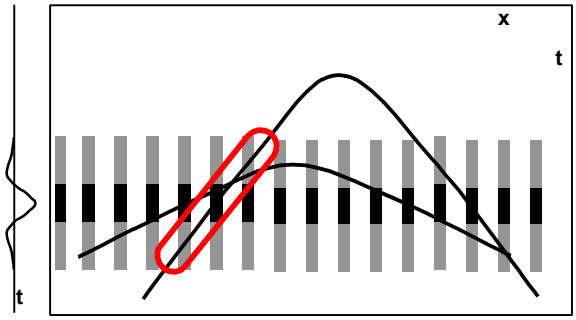

Figure 6. Reduction of aliased energy by low pass filtering.

This low pass filtering is accomplished by defining a filter that varies with the dip of the diffraction as illustrated in Figure 7. The width of the diffraction illustrates the period or width of a filter that is required to lowpass filter the data below that part of the diffraction. Now the summation across the event will tend to zero. .

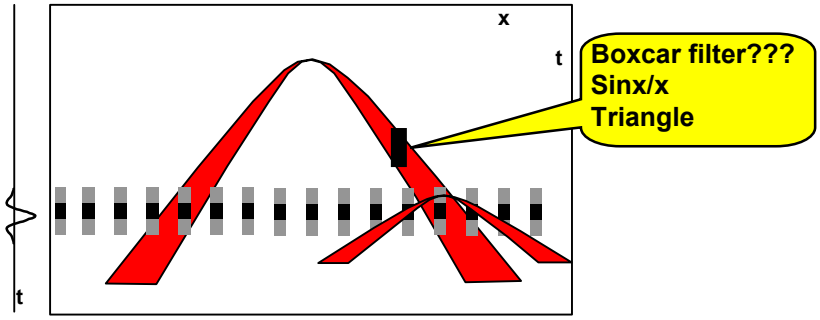

Figure 7. A diffraction dependent lowpass filter.

Note that diffractions at different locations will have different slope when they intersect the same area of the event. Consequently, the data at a given location must be filtered each time it is summed into a diffraction; a very computationally intensive process. We call this diffraction filter the antialiasing filter (AAF).

THE ALIASING EQUATION

The cutoff frequency F_c of the antialiasing filter depends on the local dip on the diffraction θ, the trace spacing δx, and the velocity V according to equation (1),

$$F_c = \frac{V}{4\,\delta x \tan\theta}. \tag{1}$$

THE FOURIER TRANSFORM DOMAIN

We now consider the 2-D Fourier transform of the horizontal event as displayed in Figure 8. The origin in this figure is the upper right corner, and the spatial Nyquist wavenumber is in the center. This view allows evaluation of aliased energy as it crosses the Nyquist "boundary".

Assume δx = 25 m, δt = 0.004 ms, V = 3000 m/s, then $\delta z = \delta t\ V/2$ = 6 m. The spatial-Nyquist wavenumber is $k_{xn} = 1/2\delta x = 0.0200\text{m}^{-1}$. The depth-Nyquist wavenumber is $k_{zn} = 1/2\delta z = 0.084\text{m}^{-1}$ corresponding to a Nyquist frequency of 125 Hz. Figure 8 has been correctly scaled to these parameters to accurately define the angle of the dipping energy. The horizontal energy is confined below the vertical axis below the origin.

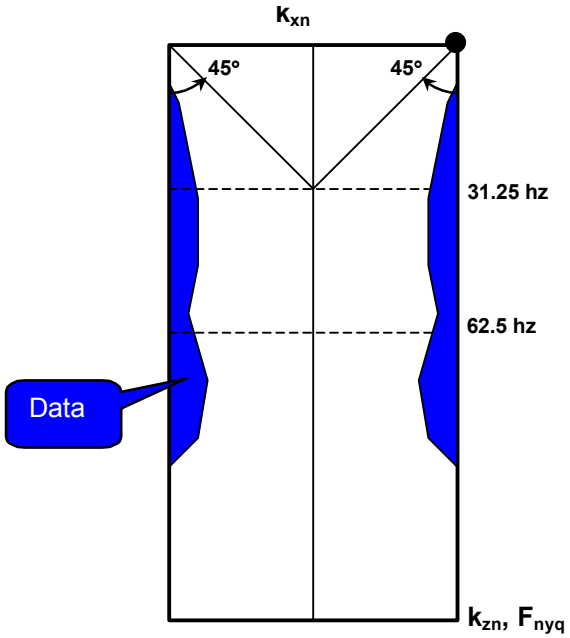

Figure 8. The Fourier transform of the horizontal event.

Let the diffraction be represented by a straight-line approximation in the time and Fourier transform domain of Figure 9 and 10.

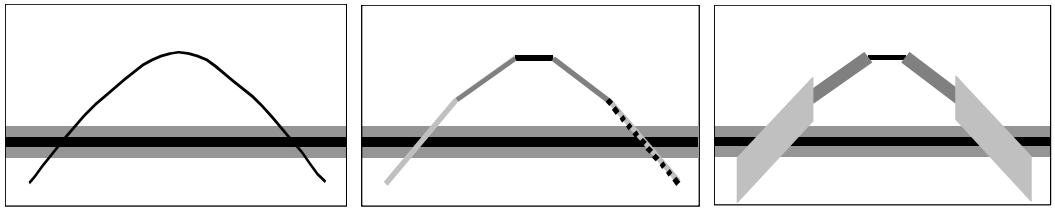

a) Diffraction b) linear diffraction c) AAF linear diffraction

Figure 9. Diffraction a) in the time domain, b) linearized, and c) showing the period of the AAF's

Summing energy below the dip in the time domain is comparable to summing energy below the dip in the frequency domain. The thicknesses of the lines in Figure 9c represent the thickness of the AAF period. (The larger the wavelet, the lower the cut-off frequency).

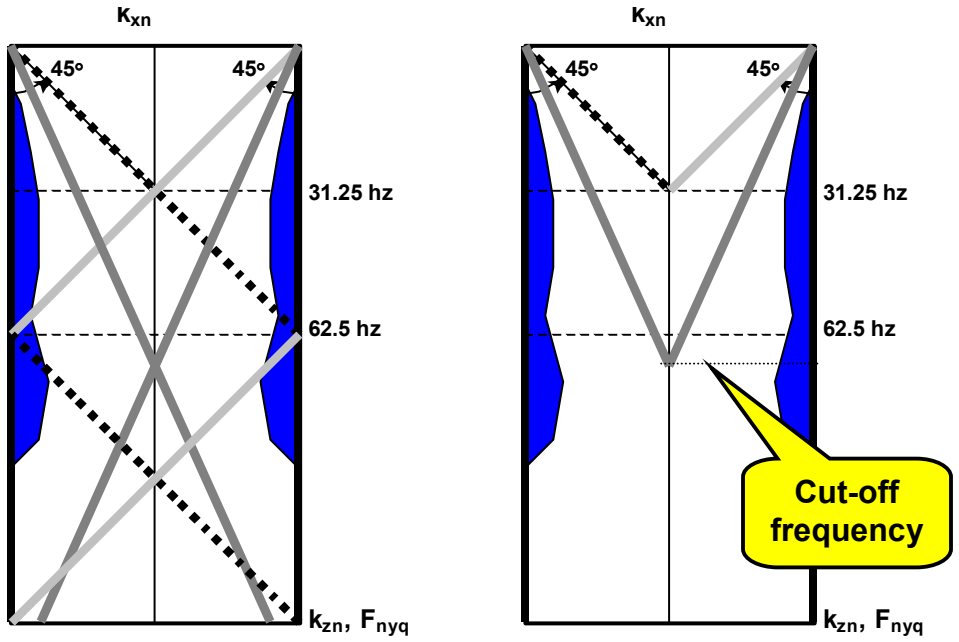

a) Aliased operator b) Anti-aliased operator

Figure 10. Fourier transform domain showing the diffraction a) with aliased energy, and b) with the AAF's applied to the aliased energy.

In the transform domain, the unfiltered dips of the diffraction extend to the maximum frequency. The steeper dips are aliased as illustrated in Figure 10a as they cross the spatial Nyquist line in the center of the figure. The steeper dips, (light gray and dashed) extend beyond the sides of the figure and re-enter on the other side (wrap-around). These aliased parts of the diffraction will pick up zero-dip energy and will place it at the apex of the diffraction, a point above the actual event.

A dip dependent high-cut filter that is applied to the aliased dips could prevent aliasing as illustrated in Figure 11b. These frequency domain filters are comparable to the filters in Figure 9c.

The above illustrations only used zero-dip data. Normal data has many more dips and their energy would also be picked up by the aliased diffraction.

One efficient approximation to the AAF divides the slopes of the diffractions into segments as illustrated again in Figure 11.

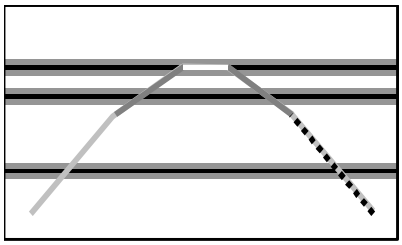

Figure 11. Section with horizontal events with a linearized diffraction.

The input data may be high-cut filtered a number of times, corresponding to the number of linear dip segments on the diffraction, three in Figure 11, giving the three filtered sections in Figure 12.

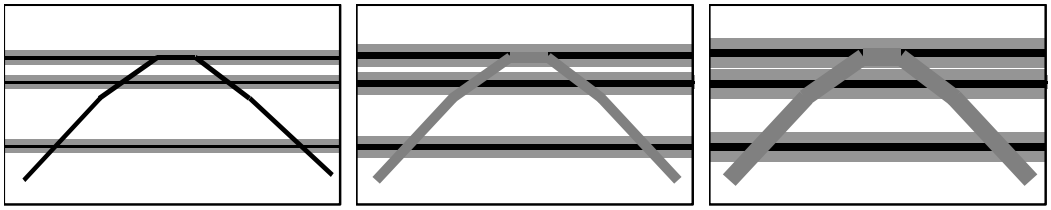

a) b) c)

Figure 12. Sections filtered for a) horizontal dips, b) intermediate dips, and c) large dips.

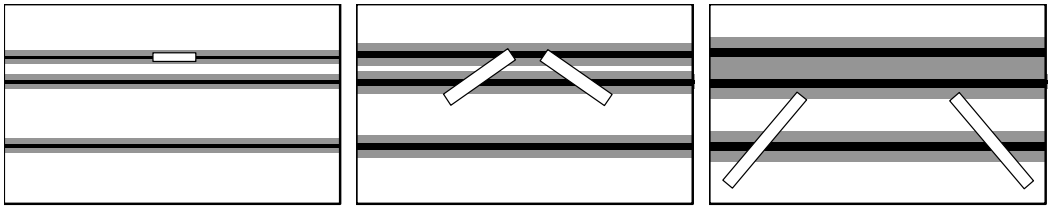

a) b) c)

Figure 13. Portions of the sections that contribute to the summed energy in the diffraction.

When summing the energy under the diffraction, the algorithm defines a dip range, then goes to the appropriate filtered section where it then picks up the appropriate energy as illustrated in Figure 13. Note the low frequency in the lower event of (c). From five to twenty-five filtered sections may be used in practical implementations. The computation and storage of this data may be expensive.

No AAF dip filter is actually required when the Kirchhoff operator dip is below a defined value (Figure 12a). That value is calculated using equation (1).

COMMENTS AND CONCLUSIONS

The AAF is computationally expensive and there are many approximations and shortcuts to reduce this expense. Quite often the AAF filter is completely ignored and may create excessive noise. Choice of an AAF may be a compromise between:

- acceptable noise,
- frequency content, and
- energy content of the dipping events.

APPENDIX

Figure A1 has been included to illustrate the exclusion and inclusion of the AAF. The left side of the figure had the AAF's turned off and the resulting aliased noise can be observed. This noised is removed from the right side of the section when the AAF's are turned on.

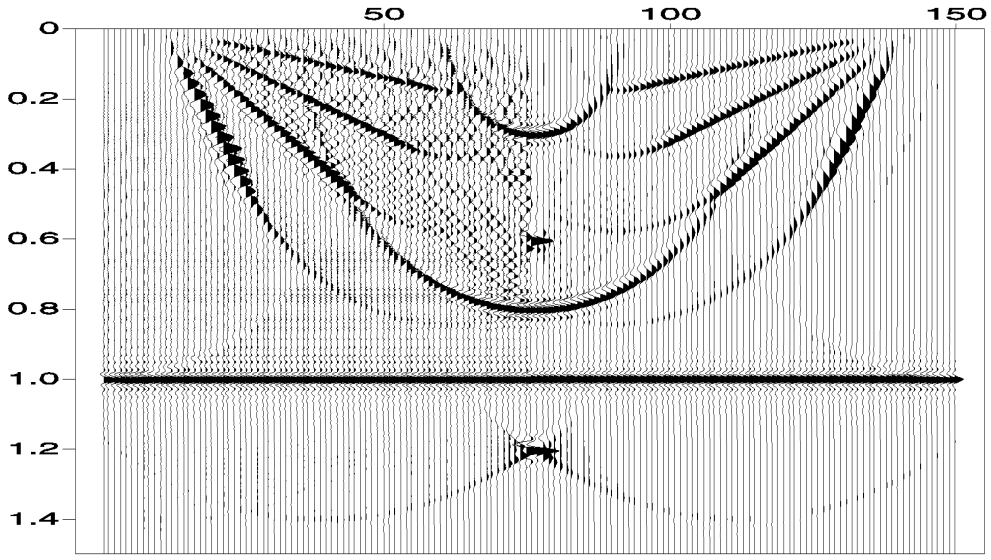

Figure A1. A Kirchhoff migration with no AAF on the left side. An AAF filter was used to produce the right side of the section.

The AAF's used on the right side in this example used computationally intensive sinx/x filters and the processing required twenty times the processing time as the left side of the section. Box car and triangular AAF's only required 3 times the processing time, but attenuated more energy on the steeper dips.

Another interesting feature of Figure A1 is the amplitude of the steeply dipping event on the left side of the section. The energy of this event, (on the input section), is aliased and this aliased energy is picked up by the aliased diffraction operator, which then produces aliased migrated energy. (The comparable dip on the right side

contains un-aliased energy with a sharp cutoff at the Nyquist boundary.) Use of the AAF's becomes a choice between aliased noise, frequency content, and processing time.

The interpolation of traces reduces the size of δx allowing the Nyquist frequencies of the AAF's to be increased, and thus reducing the amount of aliasing. Optimally, the trace spacing can be chosen to allow all dips to a maximum of 45 degrees (all input data to migration), to be migrated without AAF's.